Convenient analytical formula for cluster mean diameter and diameter dispersion after nucleation burst

M. Tacu [1] A. Khrabry [2,*] and I. D. Kaganovich [2]

[1]*École Normale Supérieure Paris-Saclay, 94230 Cachan, France*
[2]*Princeton Plasma Physics Laboratory, Princeton University, Princeton, New Jersey 08543, USA*

We propose an alternative method of estimating the mean diameter and dispersion of clusters of particles, formed in a cooling gas, right after the nucleation stage. Using a moment model developed by Friedlander [S. K. Friedlander, Ann. N. Y. Acad. Sci. **404**, 354 (1983)], we derive an analytic relationship for both cluster mean diameter and diameter dispersion as a function of two of the characteristic times of the system: the cooling time and the primary constituents collision time. These formulas can be used to predict diameter and dispersion variation with process parameters, such as the initial primary constituents' concentration or cooling rate. It is also possible to use them as an input to the coagulation stage, without the need to compute complex cluster generation during the nucleation burst. We compared our results with a nodal code (NGDE) and got excellent agreement.

I. INTRODUCTION

Nanoparticle formation has attracted much interest in the last decades. For numerous environmental and industrial applications using these nanosized particles [1,2], it is important to control, among other parameters, the mean particle size and the width of the size distribution.

In the case of a cooling and expanding gas, like the one we consider in this paper, which could be for example laser ablated [3], created by plasma arc [4,5] or dielectric barrier discharge [6], we can distinguish two main stages of nanoparticle evolution [7]: the nucleation and growth stage. Each of these stages will have a different impact on the particle size distribution.

In the nucleation stage, as the initially nonsupersaturated gas cools down, the vapor saturation pressure decreases below the gas pressure and the cluster formation process begins. With further temperature drop, this process intensifies as the saturation pressure decreases precipitously with the temperature, faster than gas pressure. The supersaturated gas returns to equilibrium via the nucleation burst, a phase of rapid cluster and droplet nucleation, when the barrier to their formation can be overcome at sufficiently low temperature. In this stage the particle size distribution will evolve from a monodisperse function (only primary constituents at the beginning) to usually a lognormal distribution [8].

Once a substantial amount of clusters is formed and most of the monomers (primary constituents) consumed, the growth stage begins, in which the clusters grow, essentially by merging with each other in the liquid phase or agglomerating in the solid phase, a process named coagulation [9]. In this stage, the particle size distribution will generally evolve in a self-similar way [9,10].

We know, since pioneering Girshick's works [11,12], that the final diameter of nanoparticles formed in a cooling gas after the nucleation stage is affected by the gas concentration and cooling rate. However, a quantitative relationship has been missing. This paper aims at obtaining analytical formulas which allow a direct computation of the first two moments of the size distribution.

Let us introduce notations and derive the nucleation rate using classical nucleation theory (CNT) [13–15]. CNT has its limitations [16–18], mainly because of applying bulk macroscopic properties to small clusters. These properties, such as the surface tension for example, are not well defined for clusters containing only a few atoms [19]. However, it is still a convenient tool for making quantitative predictions [20] and our results do not depend much on the nucleation rate as we will see further.

During the nucleation stage, small clusters form first and then grow by absorbing more and more monomers. However, the formation of small clusters is energetically unfavorable. There is an energy barrier [21] $\Delta\Phi = \Phi - \Phi_0$, where Φ is the thermodynamic potential of the system {vapor, liquid droplets} and Φ_0 the potential of the system before the liquid droplet formation. The change in the potential due to the cluster (droplet) formation is

$$
\begin{aligned}
\Delta\Phi &= \mu_l n_l + \mu_g n_g + 4\pi r^2 \gamma - \mu_g(n_g + n_l) \\
&= -(\mu_g - \mu_l)n_l + 4\pi r^2 \gamma \\
&= -\frac{\mu_g - \mu_l}{N_A}N + \epsilon_s N^{2/3}.
\end{aligned}
\tag{1}
$$

Here, N is the number of monomers in the cluster, n_l and n_g are the amount of liquid and gas, in moles, in the final state (the total amount of matter $n_g + n_l$ is conserved), r is droplet's radius, and N_A is the Avogadro number. The molar liquid

---

*Present address: Lawrence Livermore National Laboratory (LLNL), Livermore, California 94550, USA.
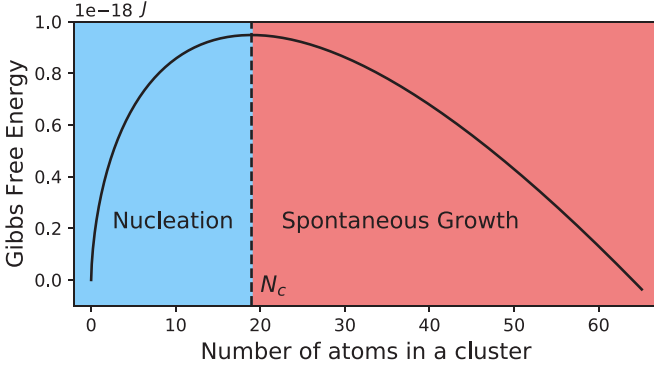
FIG. 1. $G(N)$, the Gibbs free energy of formation of a cluster containing N atoms as a function of N.

chemical potential is denoted by μ_l and the gas chemical potential by μ_g.

The first term on the right-hand side (RHS) corresponds to the binding energy of atoms within the liquid volume. The second is proportional to $N^{2/3}$ and corresponds to the surface energy. The constant of proportionality is ϵ_s, the specific surface energy of the cluster, which can be deduced from the surface tension coefficient γ, by $\epsilon_s = 4\pi r_W^2 \gamma$, where r_W is the Wigner-Seitz radius defined so that $4\pi r_W^3 \rho / 3m_a = 1$ and ρ is the mass density of liquid with m_a being the mass of a monomer.

For an ideal gas and incompressible liquid, the chemical potential difference can be written [22] by introducing Boltzmann's constant k: $\mu_g - \mu_l = kTN_A\ln(S)$, where the supersaturation degree S is defined using n_1, the monomer number density in the gas, and n_{sat}, the number density corresponding to saturation conditions

$$S = \frac{n_1}{n_{\text{sat}}}. \tag{2}$$

The second term of the RHS has an opposite sign to the first ($S > 1$) because of the binding energy reduction for atoms near the cluster's surface.

We define the initial time $t = 0$, so that $S = 1$ at that moment and we set $n_0 \equiv n_{\text{sat}}(t = 0) = n_1(t = 0)$. The saturation particle density is then given by Clausius-Clapeyron law:

$$n_{\text{sat}}(T)T = n_0 T_0 e^{\frac{e_a}{k}\left(\frac{1}{T_0} - \frac{1}{T}\right)}, \tag{3}$$

where T is the actual temperature and e_a is the vaporization energy per atom for a flat surface.

In our case, Φ is the Gibbs free energy $G(N)$, the typical profile of which is shown in Fig. 1. The function is nonmonotonic, for small clusters the free surface energy dominates over the binding energy, $G(N)$ is growing with N. At some value of N, commonly referred as the critical number N_c, the function reaches its maximum and then monotonically decreases. Corresponding cluster size is called critical cluster diameter $d_{cl}^* = 2r_W N_c^{1/3}$:

$$d_{cl}^*(S, T) = r_W \frac{4\theta}{3\ln S}, \tag{4}$$

where $\theta = e_s/kT$ is the dimensionless surface energy.

In other words, for small clusters, with a number of atoms less than N_c, growth is energetically unfavorable (attachment
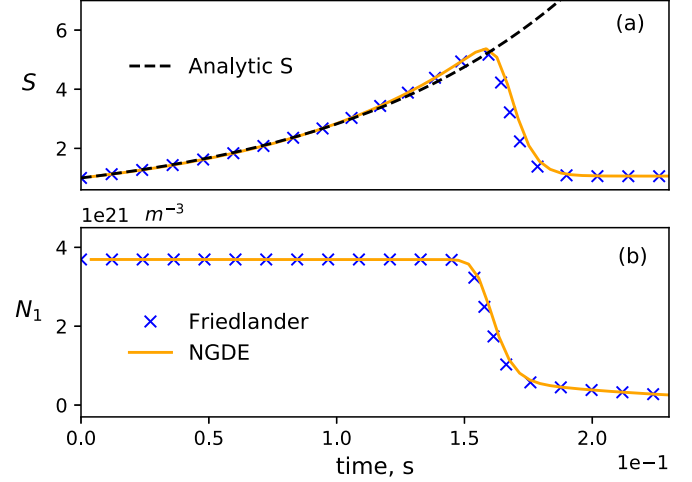
FIG. 2. (a) S as a function of time for aluminum with $\dot{T}_0 = 10^3$ K/s, $T_0 = 1773$ K, and $\gamma = 0.948$ N/m calculated with Friedlander's model (crosses), NGDE code using 41 nodes (solid line), and analytic S from Eq. (7) (dashed line). (b) n_1 in the same conditions as (a).

of each next atom to the cluster results in the Gibbs energy increase), but for larger clusters with a number of atoms larger than N_c, the cluster growth is energetically favorable. Hence, once a cluster has reached the critical size, it will spontaneously grow by consuming the gas monomers, absorbing them on its surface. This is why the nucleation rate J plays such an important role in CNT. It gives us the rate of production of particles of critical size d_{cl}^* which will inevitably grow. In order to derive it we could notice that it will be proportional to the exponential of $-G(N_c)/kT = 4\theta^3/27\ln(S)^2$, the energy barrier that a cluster needs to overcome (by thermal fluctuations) in order to reach the critical size. The proportionality coefficient, however, is still subject to debate [18]. As already said, CNT has a number of limitations. The capillarity approximation, which extends bulk thermodynamic properties to nanoscale clusters, leads to errors in estimating the free energy of small clusters. There were several attempts to correct this problem [14], but the most consistent correction is Girshick's one [14,20] that leads to the following nucleation rate:

$$J = n_1 n_{\text{sat}} v_1 e^{\theta} \sqrt{\frac{2\gamma}{\pi m_a}} e^{-4\theta^3/27\ln(S)^2}. \tag{5}$$

Since we only consider short nucleation stage, the nucleation rate can be simplified. We assume a constant gas cooling rate $\dot{T}_0$ and a linear decrease of temperature:

$$T(t) = T_0 - \dot{T}_0 \times t. \tag{6}$$

As expected, the supersaturation degree increases with time since n_1 remains nearly constant [see Fig. 2(b), no monomer consumed yet], but saturated gas density n_{sat} decreases with temperature [see Eq. (3)]. According to this picture, we can approximately write using Eq. (3) (with $n_1 \approx n_0$ and $T \approx T_0$) $\ln(n_0/n_{\text{sat}}) \approx \frac{e_a \dot{T}_0}{kT_0^2}t$, which allows us to express the

supersaturation [see Fig. 2(a)]

$$S(t) \approx \begin{cases} \exp\left(\frac{e_a \dot{T}_0}{kT_0^2} t\right), & t < t_0 \\ 1, & t > t_0. \end{cases} \quad (7)$$

Here, t_0 is the time at which the nucleation burst occurs (at the maximum of S), or simply nucleation time, when nearly all monomers are quickly consumed into clusters.

If we use Eq. (7) and suppose a sufficiently small t_0 such that $\dot{T}_0 t_0 / T_0 \ll 1$, an assumption that will be discussed further, we can write $G(N_c)/kT \approx b/t^2$, with $b = 4\theta_0^3 (kT_0)^4 / 27(k e_a \dot{T}_0)^2$, where $\theta_0 = \theta(t=0)$. The nucleation rate will then read as, for times such as $t < t_0$,

$$J \approx n_1 n_{\text{sat}} v_1 e^{\theta_0} \sqrt{\frac{2\gamma}{\pi m_a}} e^{-b/t^2}. \quad (8)$$

With this approximation, the abrupt nucleation process seems clearer now. The nucleation rate will only have substantial values near t_0, when the critical barrier to particle nucleation d_{cl}^* will be sufficiently low. In the case of a cooling gas, the nucleation rate is acting thus as a switch.

In the next section we link supersaturation variations with the nucleation rate via Friedlander's model.

II. FRIEDLANDER'S MODEL

During the short nucleation stage, the coagulation process can be neglected because it happens on a much longer timescale than the evaporation or condensation process [9]. Furthermore, we suppose being in the free molecule size range [10], meaning that the mean free path in the gas is much greater than the mean particle diameter. This is particularly true at the beginning of the nucleation, even at atmospheric pressure, since only monomers are present. In this case, it is reasonable to assume that the main mechanism of growth of particles above the critical size is monomer deposition on their surface. The diameter of all clusters such that $d_{cl} > d_{cl}^*$ will then grow [9] at a rate proportional to the net condensation flux, which is determined by the difference between condensation and evaporation:

$$\frac{d(d_{cl})}{dt} = 2(n_1 - n_{\text{sat}}) v_1 v_{th}, \quad (9)$$

where $v_1 = 4\pi r_W^3 / 3$ is the the average volume in liquid per monomer and $v_{th} = \sqrt{\frac{kT}{2\pi m_a}}$ is the thermal velocity of the monomers.

The growth law given in the equation above is an approximation, only valid in the nucleation stage and in the case where the nucleation and coagulation processes are decoupled (as in a cooling gas, for example). It is also usually a function of the diameter, especially in the coagulation stage. When two clusters agglomerate or merge, the final diameter is a function of the diameter of each particle. It is thus remarkable for the growth law to be independent of the diameter. We will use this property further, to close the moment model.

Let us denote by $f(d_{cl}, t)$ the particle size distribution, where d_{cl} is the particle diameter. Let also n_{cl}, M_1, and A be its first three moments :

$$n_{cl} \equiv \int_{d_{cl}^*}^{\infty} f(d_{cl}) d(d_{cl}),$$

$$M_1 \equiv \int_{d_{cl}^*}^{\infty} d_{cl} f(d_{cl}) d(d_{cl}),$$

$$A \equiv \int_{d_{cl}^*}^{\infty} \pi d_{cl}^2 f(d_{cl}) d(d_{cl}). \quad (10)$$

Here, n_{cl} is the number density of clusters above the critical diameter, A relates to average surface area of clusters above the critical diameter, and $M_1 = \langle d_{cl} \rangle n_{cl}$ is the average diameter of clusters above the critical diameter.

In order to find the time behavior of the moments, we will make use of the kinetic equation that expresses the change of $\partial f / \partial t$ by the evaporation or condensation process. For clusters big enough (say with more than 10 monomers), this equation can be written [9] in the continuous form as $\partial f / \partial t + \partial I / \partial d_{cl} = 0$, where $I(d_{cl}, t)$ is the particle current, or the rate of production of particles of size d_{cl} at the time t.

In the free molecule size range, we can approach the particle current with $I = f d(d_{cl})/dt$, as explained in Ref. [9]. We also notice that with our definition of I, the nucleation rate can be expressed as $J = I(d_{cl}^*, t)$. Making use of the equations above, as well as of Eq. (9), we compute the time derivative of A by integration by parts following Friedlander:

$$\frac{dA}{dt} = \int_{d_{cl}^*}^{\infty} 2\pi d_{cl} \frac{d(d_{cl})}{dt} f d(d_{cl})$$
$$+ \pi d_{cl}^{*2} J - \pi d_{cl}^{*2} f(d_{cl}^*) \frac{d(d_{cl}^*)}{dt}. \quad (11)$$

The term proportional to $f(d_{cl}^*) d(d_{cl}^*)/dt$ can be neglected since at the beginning of the nucleation $f(d_{cl}^*)$ is small and at the nucleation burst $d(d_{cl}^*)/dt$ vanish because of S reaching its maximum. We proceed in the same way for the other moments to obtain

$$\frac{dA}{dt} = a_1 N_c^{2/3} J + 4\pi v_1 v_{th} (n_1 - n_{\text{sat}}) M_1, \quad (12)$$

$$\frac{dM_1}{dt} = 2 r_W N_c^{1/3} J + 2 v_1 v_{th} (n_1 - n_{\text{sat}}) n_{cl}, \quad (13)$$

$$\frac{dn_{cl}}{dt} = J, \quad (14)$$

where $a_1 = 4\pi r_W^2$ is the average surface in liquid per monomer.

Equations (12) and (13) describe the evolution of the cluster's average area and diameter. The first term in the RHS stands for formation of new critical size clusters, the second term in the RHS accounts for the surface deposition. Equation (14) describes the evolution of n_{cl} by critical size cluster formation at a rate J (again only clusters above critical size are considered in n_{cl}).

Since we consider monomer deposition as being the main process of cluster growth, we need a monomer balance to account at the same time for their consumption at a rate $N_c J$ and for their deposition on the surface of clusters, which

happens at a rate $v_{th}(n_1 - n_{\text{sat}})A$:

$$\frac{dn_1}{dt} = -N_c J - v_{th}(n_1 - n_{\text{sat}})A. \qquad (15)$$

Equations (12)–(15) are the so called Friedlander's model describing the behavior of the monomer concentration, as a function of time in our case, since the temperature is time dependent. In the case of a cooling gas, this model can be simplified.

To do so, let us write the monomer balance in terms of the supersaturation S given in Eq. (7). We use $\frac{1}{n_{\text{sat}}}\frac{dn_{\text{sat}}}{dt} = \frac{\dot{T}_0}{T}(1 - \frac{e_a}{kT}) \approx -\frac{e_a \dot{T}_0}{kT_0^2}$ and neglect the nucleation term as we explain in the Appendix to get

$$\frac{dS}{dt} - \frac{e_a \dot{T}_0}{kT_0^2}S + (S-1)v_{th}A = 0. \qquad (16)$$

At the beginning of the cooling, A is small because the critical size is infinite (S close to 1) and clusters can not durably form via monomer attachment. The term containing A is then small and can be neglected which results in an exponential growth of S. When A becomes sufficiently big, the middle term can be neglected. We obtain then an equation on $S - 1$, which rapidly decreases to 0. This behavior can be recovered by numerical simulations in Fig. 2(a).

Further, we replace n_1 with n_0 before the nucleation burst as we did to derive Eq. (7). The decreasing temperature in the gas makes the nucleation process very abrupt, so that the monomers are not consumed at the beginning of the condensation. There is a high energy barrier that the small clusters need to overcome to grow and thus consume monomers. Let us assume that $n_1 \approx n_0$ and neglect nucleation terms (see Appendix). This allows us to simplify Friedlander's model as follows:

$$\frac{dS}{dt} - \frac{e_a \dot{T}_0}{kT_0^2}S + (S-1)v_0 A = 0,$$
$$\frac{dA}{dt} = 4\pi V_1 v_0 (n_0 - n_{\text{sat}})M_1,$$
$$\frac{dM_1}{dt} = 2V_1 v_0 (n_0 - n_{\text{sat}})n_{cl},$$
$$\frac{dn_{cl}}{dt} = n_0 n_{\text{sat}} V_1 e^{\theta_0}\sqrt{\frac{2\gamma}{\pi m_a}}e^{-b/t^2}. \qquad (17)$$

Here, we replaced v_0 with $v_{th}(t = 0)$ because v_{th} is a slowly varying function of T.

Numerical simulations confirm that this model is accurate up to the nucleation time. However, we still have to get further in our approximations in order to find an expression of t_0; this is the object of the next section.

III. ANALYTIC EXPRESSION FOR NUCLEATION TIME

In this section we give an analytic expression to the crucial parameter that describes the nucleation stage: the nucleation time t_0. Because of the abruptness of the nucleation event [12], this time will also give us an estimate of the time at which the transition process between nucleation and coagulation starts.

Even if Eq. (17) is a simplified version of Friedlander's model, it is still impossible to integrate it analytically because
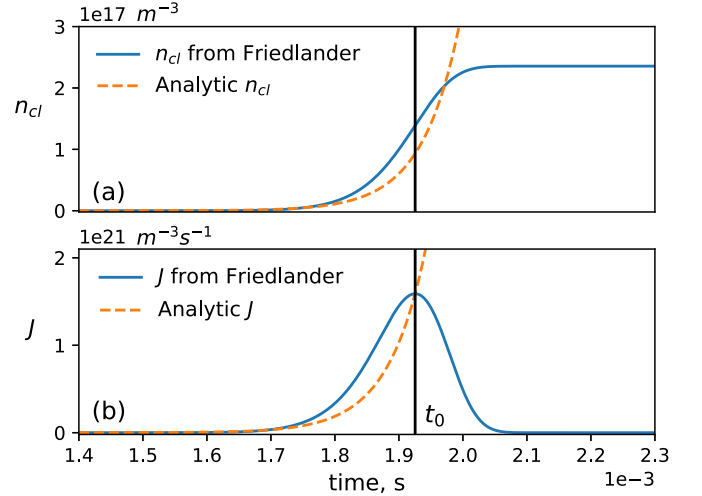
FIG. 3. (a) The total concentration of clusters above critical size n_{cl}, for $\dot{T}_0 = 10^5$ K/s and $T_0 = 1773$ K. (b) Nucleation rate J from Friedlander and from Eq. (18).

of the nucleation rate which is proportional to e^{-b/t^2}. In order to integrate the system, we will approximate the nucleation rate near t_0 as an exponential function. We write $b/t^2 \approx b/t_0^2 - 2b(t - t_0)/t_0^3$, so that

$$J(t) \approx J(t_0)e^{-2b(t-t_0)/t_0^3}. \qquad (18)$$

Now, we can explicitly find n_{cl}, M_1, A, and S by direct integration of Eq. (17). We see from Fig. 3 that J is not exactly an exponential function and integrating J three times to get A leads to greater errors than those we see for n_{cl}. We will, however, continue since the area under the nucleation rate is well approximated by the exponential function in the equation above and the sharp increase in J ensures us that its amplitude will hardly affect t_0. This will allow us to replace n_{sat} in the coefficient of the nucleation rate with n_0, so that $J(t_0)$ becomes

$$J(t_0) = n_0^2 V_1 e^{\theta_0}\sqrt{\frac{2\gamma}{\pi m_a}}e^{-b/t_0^2}. \qquad (19)$$

We also replace $n_0 - n_{\text{sat}}(t)$ with $n_0 - n_{\text{sat}}(t_0) \approx n_0$ since we develop near t_0 and because the coefficients of the moments in Eq. (17) have a slower variation in time than the moments themselves.

Replacing the coefficients by their value at t_0 allows us to analytically integrate Eq. (17). First, it transforms into the system

$$\frac{dS}{dt} - \frac{e_a \dot{T}_0}{kT_0^2}S + (S-1)v_0 A = 0,$$
$$\frac{d^3 A}{dt^3} = 8\pi V_1^2 v_0^2 n_0^2 J(t_0)e^{2b(t-t_0)/t_0^3}. \qquad (20)$$

Then, by neglecting the terms in $e^{-2b/t_0^2} \ll 1$ while integrating A:

$$A(t) = 8\pi V_1^2 v_0^2 n_0^2 J(t_0)\left(\frac{t_0^3}{2b}\right)^3 e^{2b(t-t_0)/t_0^3}. \qquad (21)$$
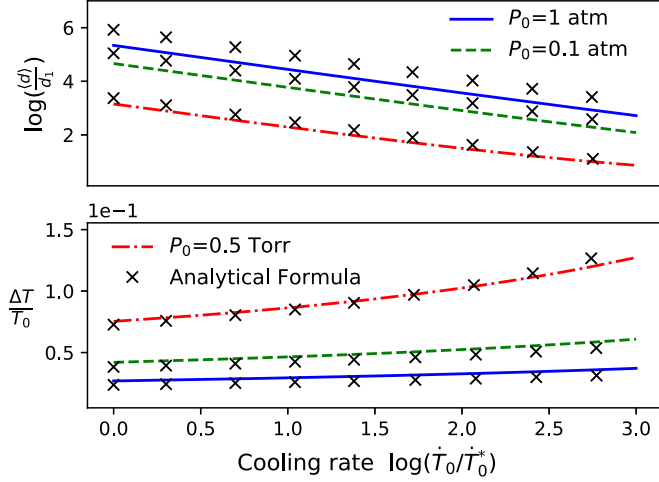
FIG. 4. (Upper) Comparison between the results given by analytic diameter from Eq. (32) (crosses) and the diameter from Friedlander's model (lines) as a function of the cooling rate with $\dot{T}_0^* = 1000$ K/s and $d_1 = 2r_W$. (Lower) $\dot{T}_0 t_0/T_0$ from Eq. (24) as a function of $\dot{T}_0$. Here $P_0 = n_0 k T_0$ and $\log_{10}$ is the natural logarithm.

From Eq. (16) with $S_{\max}$ being the maximum supersaturation degree $S(t_0)$, we get (since $S_{\max}$ is usually greater than 1)

$$A(t_0) = \frac{e_a \dot{T}_0}{kT_0^2 v_0} \frac{S_{\max}}{S_{\max} - 1} \approx \frac{e_a \dot{T}_0}{kT_0^2 v_0}. \tag{22}$$

Using both Eqs. (21) and (22) we obtain

$$t_0^9 J(t_0) = \frac{b^3 e_a \dot{T}_0}{\pi k T_0^2 v_0^3 V_1^2 n_0^2}. \tag{23}$$

The equation above is an implicit equation on t_0, which justifies *a posteriori* the approximations we had on the amplitude of the nucleation rate. The steep variations of $t^9 J(t)$ are the reason why the expression of the nucleation rate, either from CNT [16] or from kinetic nucleation theory [14], is of little importance in the determination of the nucleation burst time.

We finalize the derivation in the Appendix and obtain an expression for t_0 which uses Lambert's function W:

$$\frac{t_0}{\tau_{\text{cooling}}} = \sqrt{\frac{\theta_0}{27 W(\tau_{\text{cooling}}/\tau_{\text{collision}})}},$$

$$\tau_{\text{cooling}} = \frac{e_s T_0}{e_a \dot{T}_0}, \quad \tau_{\text{collision}} = \frac{4}{v_0 V_1^{2/3} n_0}, \tag{24}$$

where τ_{cooling} is proportional to the cooling time and $\tau_{\text{collision}}$ is the typical time of collision between monomers from kinetic gas theory.

W is a slowly varying function, thus, the main dependence of t_0 on external parameters is in the cooling rate. The temperature difference $\Delta T = T_0 - T(t_0) = \dot{T}_0 t_0$ between the beginning of the condensation and the nucleation burst will thus be almost the same for different materials and different temperatures. We also observe in Fig. 4 that $\Delta T/T_0$ is small in a wide range of $\dot{T}_0$, which confirms our initial assumption for obtaining Eq. (8).

The formula was tested for aluminum and results are presented in Fig. 4, where it is compared with predictions

TABLE I. Values of the main parameters for different materials at atmospheric pressure and corresponding Clapeyron temperature.

Material	kT_0/e_a	θ_0	e_s/e_a	$\tau_{\text{collision}}$
Al	0.08	5	0.4	3.8×10^{-8} s
Au	0.07	9	0.7	5.9×10^{-8} s
Ag	0.08	9	0.7	4.0×10^{-8} s
Cu	0.08	10	0.8	3.7×10^{-8} s
B	0.06	4	0.2	9.5×10^{-8} s

from Friedlander's model. It also shows a good agreement for other materials given in Table I. NIST database was used to compute the coefficients in the table, inferred from the basic properties of the materials.

IV. DIAMETER AND DISPERSION

In this section we express the mean particle diameter $\langle d_{cl} \rangle = M_1/n_{cl}$ and dispersion σ at the end of the nucleation stage using results from the previous section. The dispersion σ is defined as

$$\sigma^2 = \frac{A}{\pi n_{cl}} - \left(\frac{M_1}{n_{cl}}\right)^2. \tag{25}$$

In order to understand the evolution of the mean diameter and dispersion, we derive their time derivatives from Eqs. (12)–(14):

$$\frac{d\langle d_{cl} \rangle}{dt} = \frac{J}{n_{cl}}(d_{cl}^* - \langle d_{cl} \rangle) + 2v_1 v_{th} n_{\text{sat}}(S - 1),$$

$$\frac{d\sigma^2}{dt} = \frac{J}{n_{cl}^2}\left(n_{cl} d_{cl}^{*\,2} - 2M_1 d_{cl}^* - \frac{A}{\pi} + 2\frac{M_1^2}{n_{cl}}\right). \tag{26}$$

We recognize a nucleation term in the two equations and an attachment term in the mean diameter derivative.

When the nucleation has finished, J drops rapidly to 0 (see Fig. 3), so that only the mean diameter continues to grow because of monomer deposition on clusters. It eventually reaches an asymptote, when excess of the monomers from the gas phase has condensed on the clusters and S drops to 1 after the nucleation has finished. We recover this behavior from directly solving Friedlander's model as shown in Fig. 5.

The dispersion, unlike the mean diameter, will thus reach an asymptote immediately after the nucleation burst, essentially because of the uniform growth of particles above critical size. This dependence of $d\sigma/dt$ on J gives a low dispersion to Friedlander's model. It allows us to compute $\langle d_{cl} \rangle$ by neglecting the dispersion and using the total number of nucleated clusters $n_\infty = n_{cl}(t = \infty)$. At the end, almost all the monomers are attached to clusters, so that n_0/n_∞ represents the average number of monomers in a cluster. It is straightforward to deduce by conservation of matter:

$$\langle d_{cl} \rangle = \left(\frac{6V_1 n_0}{\pi n_\infty}\right)^{1/3}. \tag{27}$$

With the sharp drop in J after the nucleation burst, $dn_{cl}/dt \approx 0$ for $t > t_0$ so that n_∞ can be approximated with
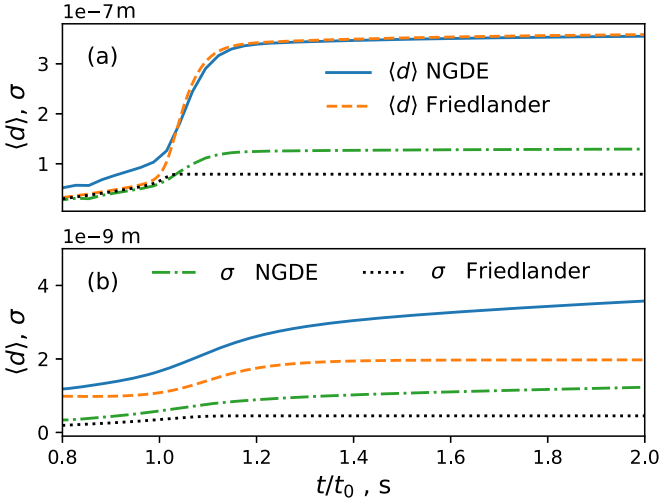
FIG. 5. (a) Comparison between the diameter and dispersion from NGDE and Friedlander, for aluminum at $\dot{T}_0 = 10^3$ K/s and $T_0 = 1773$ K. (b) Diameter and dispersion for $\dot{T}_0 = 10^6$ K/s and $T_0 = 1773$ K.

$n_{t_0} = n_{cl}(t = t_0)$ as follows:

$$n_\infty \approx n_{t_0} = \int_0^{t_0} J(t_0) e^{2b(t-t_0)/t_0^3} dt \approx \frac{t_0^3}{2b} J(t_0). \quad (28)$$

We then use Eq. (23) to replace $J(t_0)$ and obtain [with $(3^7/4)^{1/3} \approx 8$]

$$\langle d_{cl} \rangle \approx \left(\frac{12 V_1 n_0 b}{\pi t_0^3 J(t_0)} \right)^{1/3} \approx 8 \frac{k V_1 e_a v_0 n_0 \dot{T}_0 t_0^2}{e_s^2}. \quad (29)$$

Let us now derive the dispersion. Because of the fast decrease of J after the nucleation burst, $d\sigma^2/dt \approx 0$ for $t > t_0$ so that we can express the final dispersion as being the dispersion the moment of nucleation burst:

$$\sigma^2 \approx \frac{A(t_0)}{\pi n_{cl}(t_0)} - \left(\frac{M_1(t_0)}{n_{cl}(t_0)} \right)^2 = 2 V_1^2 v_0^2 n_0^2 \frac{t_0^6}{b^2} - V_1^2 v_0^2 n_0^2 \frac{t_0^6}{b^2}. \quad (30)$$

Combining Eqs. (27) and (30) yields finally

$$\frac{\sigma}{\langle d_{cl} \rangle} = \frac{27}{32} \frac{e_a}{e_s} \frac{\dot{T}_0 t_0}{T_0} \approx \frac{t_0}{\tau_{\text{cooling}}}. \quad (31)$$

We can see in Fig. 5 how $\sigma \approx \langle d \rangle$ near the nucleation burst and how different they are at the end, according to our previous discussion of Eq. (26).

Finally, we get the following expressions for the mean diameter and dispersion:

$$\frac{\langle d_{cl} \rangle}{2 r_W} = \frac{\tau_{\text{cooling}}/\tau_{\text{collision}}}{W(\tau_{\text{cooling}}/\tau_{\text{collision}})} \propto \frac{n_0}{\dot{T}_0},$$

$$\frac{\sigma}{\langle d_{cl} \rangle} = \frac{t_0}{\tau_{\text{cooling}}}. \quad (32)$$

These formulas give a quantitative explanation to a result previously observed by Girshick [11,12], namely, the linear dependence of the mean diameter on monomer concentration and the inversely proportional dependence on the cooling rate. The formulas can be used either to estimate the final cluster size and their dispersion or as an input for a coagulation

model, thus without having to compute the evaporation or condensation process.

For the materials presented in Table I, $\frac{\Delta T}{T_0} \approx 0.1$ and $e_a \approx e_s$, which gives us a dispersion an order of magnitude lower compared to the mean diameter. However, even if small, it is not zero. It is the main reason we chose the Friedlander's model over more simplified models as, for example, Nemchinski's monodisperse model [23] or Panda's model [7] accounting for both nucleation and coagulation. With this approach we can compute analytically the dispersion (neglected in Panda's model) and compare it with full codes such as NGDE [24]. The presentation of our numerical results is the object of the next section.

V. COMPARISON WITH NGDE CODE

We model the cluster evolution numerically using the NGDE code which accounts for nucleation, condensation, evaporation, and coagulation in solving the general differential equation (GDE) [9]. Modeling the entire cluster evolution is a difficult task, especially if we want to capture both the nucleation event and further cluster growth. In fact, these two processes are both on a different temporal and spatial scale. The nucleation time is very short compared to coagulation time, and coagulating particles have a volume many orders of magnitude higher than nucleating particles.

Codes such as kinetic Monte Carlo [25] which rely on counting rare events, such as first order phase transitions, are very accurate in describing the nucleation event, but fail to simulate cluster growth.

General GDE solvers are accurate because they solve all the particle evolution, but are also very computationally intensive. Approximations can be made such as replacing sums by integrals for particles bigger than a given size [12], but even then there remain numerical difficulties. In other codes, assumptions are made on the particle size distribution, such as supposing it lognormal [10] or bimodal, which is the case for some systems [8] but not for all of them [9]. NGDE is a general GDE solver that uses a logarithmic discretization of cluster volume space in nodes. This approximation makes the solution subject to numerical diffusion, especially in the case of rough discretization. However, this allows to treat at the same time nucleation and coagulation with reasonable computation times.

We performed simulations with both Friedlander's model and NGDE for an example of aluminum vapor cooling with $\dot{T}_0$ in the range 10^3–10^6 K/s and $T_0 = 1773$ K, corresponding to atmospheric saturation pressure. In Fig. 2 we see an exponential growth of S and its rapid decrease to unity, a result already observed in Refs. [7,12] and explained in the previous sections. There is a very good agreement between NGDE and Friedlander's model, which shows that agglomeration of clusters (neglected by Friedlander) does not play a significant role during the nucleation stage, at least in the free molecule size range. In Fig. 5 we compare the mean diameter and dispersion at different cooling rates. While we get a good agreement for $\dot{T}_0 = 10^3$ K/s, we see that for higher cooling rates, the diameter and dispersion continues to grow in NGDE but not in Friedlander's model. Even if the main changes are near the nucleation rate (see Fig. 6), it seems that there is a more visible
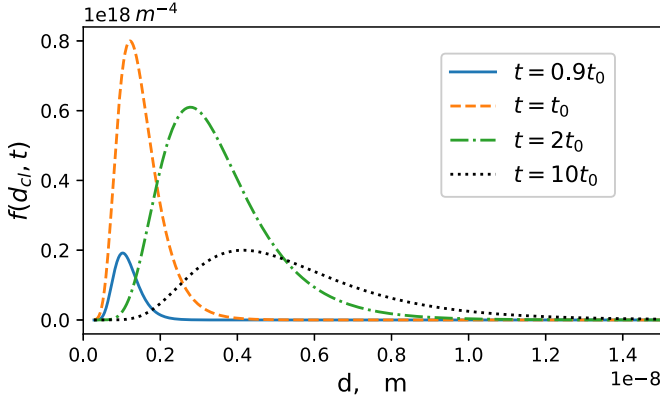
FIG. 6. Particle size distribution (primary constituents excluded), interpolated as a lognormal function from 41 points (nodes) in NGDE. Data for aluminum at $T_0 = 1773$ K, $\dot{T}_0 = 10^6$ K/s and different times.

coagulation in the case of a bigger cooling rate. To explain this behavior let us notice that the coagulation process depends on n_{cl}^2 (in the case where as an approximation, we consider a collision between all of the particles bigger than d_{cl}^*). From Eq. (27), n_{cl}^2 is bigger for smaller diameter. The mean diameter at nucleation is smaller at higher cooling rates (see Ref. [12] for the influence of the cooling rate on diameter at nucleation), meaning that there will be more clusters in the collision stage and thus a more visible coagulation. In a real gas, several effects such as the dependence of the particle size distribution on the volume of the system [26] or the carrier gas effect on the nucleation and especially coagulation have to be taken into account. Since we consider applications to plasma arcs or dielectric barrier discharges, the first effect was neglected. Using Wedekind's work [27] to change the nucleation rate we found the carrier gas to play a negligible role. We conclude that the thermalization with the carrier gas is sufficiently rapid [28] to keep nucleation under isothermal conditions.

VI. CONCLUSION

In this paper we study the nucleation stage in a cooling gas. We recall the derivation of Friedlander's model in the case of a uniform growth of clusters bigger than the critical size. If the cooling rate is typically smaller than 10^6 K/s, monomer consumption by nucleation can be neglected with respect to monomer deposition on clusters and the nucleation rate can be approximated by an exponential function.

Using this approximation, we derive an analytical formula, for the time at which the nucleation of critical particles reaches its maximum, or the nucleation burst. With this formula and matter conservation we derive analytical formulas for both mean diameter and its dispersion immediately after the nucleation stage, as a function of the cooling time and collision time between gas particles.

We found that the mean diameter is proportional to the initial monomer concentration and inversely proportional to the cooling rate. We also found that for big cooling rates the nucleation stage and the coagulation stage are not so well separated. We compared our analytical results with a nodal

code (NGDE) and Friedlander's model, for cooling rates in the range 10^3 to 10^6 K/s and got excellent agreement.

APPENDIX

Let us show that for reasonable cooling rates (typically $\dot{T}_0 < 10^6$ K/s) we can neglect the nucleation terms with respect to the deposition terms (containing $n_1 - n_{sat}$). Since $n_{cl} = \int_0^\infty J(t)dt$ and J is varying over a small time δt, we can write $n_{cl} \approx J\delta t$, then, near the nucleation burst ($t = t_0$) in Eq. (17),

$$N_c J \ll v_{th}(n_1 - n_{sat})A \approx v_{th}n_0 a_1 n_{cl} \approx v_{th}n_0 a_1 J\delta t. \quad \text{(A1)}$$

Neglecting $N_c J$ with respect to $v_{th}(n_1 - n_{sat})A$ is thus equivalent to showing that $N_c \ll v_{th}n_0 a_1 \delta t$. Here, $v_{th}n_0 a_1 \delta t$ is the number of particles attached to a cluster during the nucleation burst (during δt). For low cooling rates this number is bigger than the critical number at the nucleation burst (where N_c reaches its minimum).

Actually, during the nucleation burst a lot of clusters of critical size are formed and grow essentially from monomer attachment, so the number of monomers that can attach to a particular cluster during this time, or $v_{th}n_0 a_1 \delta t$ should be much bigger than N_c, the number of monomers in a nucleated cluster. Numerical simulations confirm this idea. If we compare the ratio between $v_{th}n_0 a_1 \delta t$ and N_c, we find for aluminum at $T_0 = 1773$ K: $v_{th}n_0 a_1 \delta t / N_c \approx 10$ for $\dot{T}_0 = 10^6$ K/s, and $v_{th}n_0 a_1 \delta t / N_c \approx 1000$ when $\dot{T}_0 = 10^3$ K/s, as expected.

Analytical time derivation. We could find the nucleation time numerically from Eq. (23), but we notice with $J(t_0) = n_0^2 v_1 e^{\theta_0}\sqrt{\frac{2\gamma}{\pi m_a}}e^{-b/t_0^2}$ that

$$\left(\frac{b}{t_0^2}\right)^{9/2} e^{b/t_0^2} = \frac{b^{3/2}n_0^4 v_1^3 v_0^3 kT_0^2 e^{\theta_0}}{e_a \dot{T}_0}\sqrt{\frac{2\pi\gamma}{m_a}}. \quad \text{(A2)}$$

Let us raise both terms of the equation above at the power of $\frac{1}{4}$ and assume that $(b/t_0^2)^{9/8} \approx (b/t_0)^2$, and it follows

$$\frac{b}{t_0^2}e^{b/4t_0^2} = \left(\frac{4}{27}\right)^{3/8}\frac{4kT_0 v_1^{1/12}\theta_0^{9/8}e^{\theta_0/4}(2\pi\gamma)^{1/8}}{e_s v_0^{1/4}m_a^{1/8}}\frac{\tau_{\text{cooling}}}{\tau_{\text{collision}}}. \quad \text{(A3)}$$

We use the definitions of v_0, v_1, e_s, and θ_0 to obtain

$$\frac{b}{4t_0^2}e^{b/4t_0^2} = \alpha\theta_0^{1/4}e^{\theta_0/4}\frac{\tau_{\text{cooling}}}{\tau_{\text{collision}}}, \quad \text{(A4)}$$

where α is given by $\alpha = (4\pi/3)^{1/12}(4/27)^{3/8}\pi^{1/8} \approx 0.6$. We assume that $\alpha/\theta_0^{1/4}e^{\theta_0/4} \approx 1$, which we can check numerically for different materials. This approximation is poorly impacting the value of t_0 since W, Lambert's function, is slowly varying. This is why the constant before the nucleation rate is not that important in the case of a cooling gas, only its variations as a function of S are important.

Finally, we get

$$\frac{\dot{T}_0 t_0}{T_0} = \frac{kT_0}{e_a} \sqrt{\frac{\theta_0^3}{27W(\tau_{\text{cooling}}/\tau_{\text{collision}})}}.$$

(A5)

[1] M. Kulmala, Science **302**, 1000 (2003).

[2] W. J. Stark, P. R. Stoessel, W. Wohllebenb, and A. Hafnerc, Chem. Soc. Rev. **44**, 5793 (2015)

[3] F. Taccogna, J. Plasma Phys. **81**, 495810509 (2015).

[4] A. Khrabry, I. D. Kaganovich, V. Nemchinsky, and A. Khodak, Phys. Plasmas **25**, 013522 (2018).

[5] S. Yatom, A. Khrabry, J. Mitrani, A. Khodak, I. D. Kaganovich, V. Vekselman, B. Stratton, and Y. Raitses, MRS Commun. **8**, 842 (2018).

[6] J. P. Borra, J. Phys. D: Appl. Phys. **39**, R19 (2006)

[7] S. Panda and S. E. Pratsinis, Nanostruct. Mater. **5**, 755 (1995)

[8] C. G. Granqvist and R. A. Buhrman, J. Appl. Phys. **47**, 2200 (1976)

[9] S. K. Friedlander, *Smoke, Dust, and Haze: Fundamentals of Aerosol Dynamics* (Oxford University Press, Oxford, 2000).

[10] S. E. Pratsinis, J. Colloid Interface Sci. **124**, 416 (1988).

[11] S. L. Girshick, C.-P. Chiu and P. H. McMurry, Plasma Chem. Plasma Process. **8**, 145 (1988).

[12] S. L. Girshick, C.-P. Chiu, Plasma Chem. Plasma Process. **9**, 355 (1989)

[13] S. L. Girshick, C.-P. Chiu and P. H. McMurry, Aerosol Sci. Technol. **13**, 465 (1990).

[14] S. L. Girshick and C.-P. Chiu, J. Chem. Phys. **93**, 1273 (1990).

[15] F. Bakhtar, B. J. Young, J. A. White, and A. D. Simpson, J. Mech. Eng. Sci. **219**, 1315 (2005).

[16] J. L. Katz and H. Wiedersich, J. Colloid Interface Sci. **61**, 351 (1977).

[17] Steven L. Girshick, P. Agarwal, and D. G. Truhlar, J. Chem. Phys. **131**, 134305 (2009).

[18] S. L. Girshick, J. Chem. Phys. **141**, 024307 (2014).

[19] M. P. Anisimov, Russ. Chem. Rev. **72**, 591 (2003).

[20] B. E. Wyslouzil and J. Wölk, J. Chem. Phys. **145**, 211702 (2016).

[21] J. Frenkel, *Kinetic Theory of Liquids* (Dover, New York, 1955).

[22] D. W. Oxtoby and R. Evans, J. Chem. Phys. **89**, 7521 (1988).

[23] V. A. Nemchinsky and M. Shigeta, Modell. Simul. Mater. Sci. Eng. **20**, 045017 (2012).

[24] A. Prakash, A. P. Bapat, and M. R. Zachariah, Aerosol Sci. Technol. **37**, 892 (2003).

[25] S. A. Davari and D. Mukherjee, AIChE J. **64**, 18 (2018).

[26] T. Haxhimali, D. Buta, M. Asta, P. W. Voorhees, and J. J. Hoyt, Phys. Rev. E **80**, 050601(R) (2009)

[27] J. Wedekind, A.-P. Hyvärinen, D. Brus, and D. Reguera, Phys. Rev. Lett. **101**, 125703 (2008).

[28] Y. Gorbachev and S. I. Nikitin, Tech. Phys. **45**, 1538 (2000).